RELATING PROCESSING OF SELECTIVE LASER MELTED STRUCTURES TO THEIR MATERIAL AND MODAL PROPERTIES

Nicholas E. Capps[1], James S. Urban[1], Brian West[1], Cody Lough[1], Adriane Replogle[2], Troy Hartwig[3], Ben Brown[3], Douglas A. Bristow[1], Robert G. Landers[1], Edward C. Kinzel[1]

[1]Department of Mechanical and Aerospace Engineering, Missouri University of Science and Technology, Rolla, MO 65409.

[2]Lincoln University, Jefferson City, MO, 65101

[3]Kansas City National Security Campus, Kansas City, MO 64147

Abstract: Selective Laser Melting (SLM) creates metal parts by fusing powder layer-by-layer. It provides significant design flexibility and the possibility of low-volume production. The engineering properties of the printed metal are a function of the local thermal history. This creates challenges for validating Additively Manufactured (AM) parts. This paper correlates the engineering properties (density, modulus, yield strength and ultimate strength) for tensile test specimens created with different process parameters with the resonant frequencies determined using modal testing. The paper shows that yield and ultimate strengths for these specimens can be determined using modal analysis.

1. Introduction

Since its inception in the late 1980's, Additive Manufacturing (AM) has grown from a preliminary prototyping process to an engineering tool capable of producing intricate metal parts that would be difficult to produce using traditional manufacturing processes with similar mechanical properties. The ability to produce complex internal features without large increases in cost has made it possible to create strong, lightweight structures that are revolutionizing the aerospace and defense industries [1,2]. In addition to complex internal structures, AM also allows for the creation of highly detailed external geometries, making anatomically accurate knee and hip replacements possible, transforming the biomedical industry. This design flexibility, coupled with comparable material properties, makes AM an extremely cost-effective way to produce high value, mission critical parts.

A cost of the design flexibility afforded by AM is that the validation of these materials is an extremely difficult and expensive undertaking. Since the desired geometry of the part being fabricated directly effects the thermal profile, each unique part morphology creates a potentially different microstructure and part properties [3,4]. This differs from traditional machining processes where the material and geometry are independent. For example, a tensile test specimen and a solid cube, even when built using the same process parameters, will have varied thermal input histories, resulting in changes to the recrystallization of the liquid that, in turn, produce large variations in strength [1,2,5]. This variance in properties is often exacerbated in the presence of complex internal structures that are possible with AM. This is a significant issue, considering that many of the parts produced with the SLM process are mission critical, and could have catastrophic consequences if they fail, such as hip replacements for elderly patients and turbines in aircraft

engines. Because the production volume for SLM parts are typically low for mission critical applications, any material validation method must be extremely thorough.

Statistically-driven destructive testing methods are not practical for most AM design processes because the number of parts required would nullify the low-volume benefits of AM. Currently available non-destructive methods, such as Computerized Tomography (CT) scans [6,7], are extremely accurate for determining part health, but are very expensive and time consuming due to the large startup investment and are limited to testing a single part at a time. Acoustic testing is a more affordable non-destructive method that detects audible changes in the frequency when a part is struck. This method works well only if the change is large enough to be audible, and the natural damping of the structure may make any measurable frequency data too short to analyze with sufficient frequency resolution. This is less of an issue for metallic parts with higher quality factors, but is still a limiting factor of the practice. Other non-destructive testing methods, such as dye permeability testing, neutron small angle scattering, and diffuse wave spectrometry may not be applicable for solid SLM parts **[7]**

The objective of this paper is to investigate how changes in processing parameters affects the engineering properties of the printed material and to test the ability to quantify those changes using modal analysis. Modal analysis is the study of the resonant frequencies and mode shapes of mechanical systems. Resonant frequencies are natural modes of vibration, where the minimum amount of force drives the maximum response from that input - a natural mechanical amplifier [8]. These modes are a fundamental property of a structure, and are determined by material properties such as mass and Young's Modulus, as well as geometry.

In recent years, modal analysis has seen increased focus in civil engineering for damage detection and mitigation. Hearn et al showed it is possible to use changes in modal parameters such as natural frequency, damping, and mode shape to detect fatigue damage in a truss structure in a laboratory setting [9]. Although the problem becomes extremely complex as the structures grow larger and the defects become non-linear, it is possible to apply this phenomenon to civil structures such as bridges and skyscrapers, a method known as Structural Health Monitoring [10]. This paper generates empirical quantitative relationships between the processing parameters used to build several identical parts and the resulting material and modal properties. It shows that it is possible to detect bulk changes in material properties through modal analysis.

2. Experimental Approach

For this study, 60 304L stainless steel tensile test specimens (ASTM E8) were built using a Renishaw AM 250 SLM process [11]. The parts were made with 800 mm/s scan speed, 50 µm layer thickness, and 85 µm hatch spacing as nominal process parameters. For this study, the research was focused on detecting bulk defects throughout the whole part. Bulk defects are uniformly distributed cracks and voids inside the specimens that are small enough to not produce concentrated stresses at any one point in the part, and numerous enough to be captured by effective properties. The most common bulk defect encountered in SLM parts is uniform porosity caused by sub-optimal printing parameters. Specimens were printed with varying laser powers between 100 and 200 W to artificially create these bulk defects.

All 60 specimens were built on a single build plate and arranged at 45° from the build plate edge. This configuration allows line-of-sight in both planes of motion. The full layout of the build is shown below, in Fig. 1 After printing, the build plate was excited using an electrodynamic shaker and specimen responses were measured with a Laser Doppler Vibrometer (LDV). Following vibration testing, the samples were removed from the build plate using electric discharge machining. Once removed, density and mechanical properties were obtained using Archimedes' Principle with deaerated water, and tensile testing using an Instron 5969, respectively.

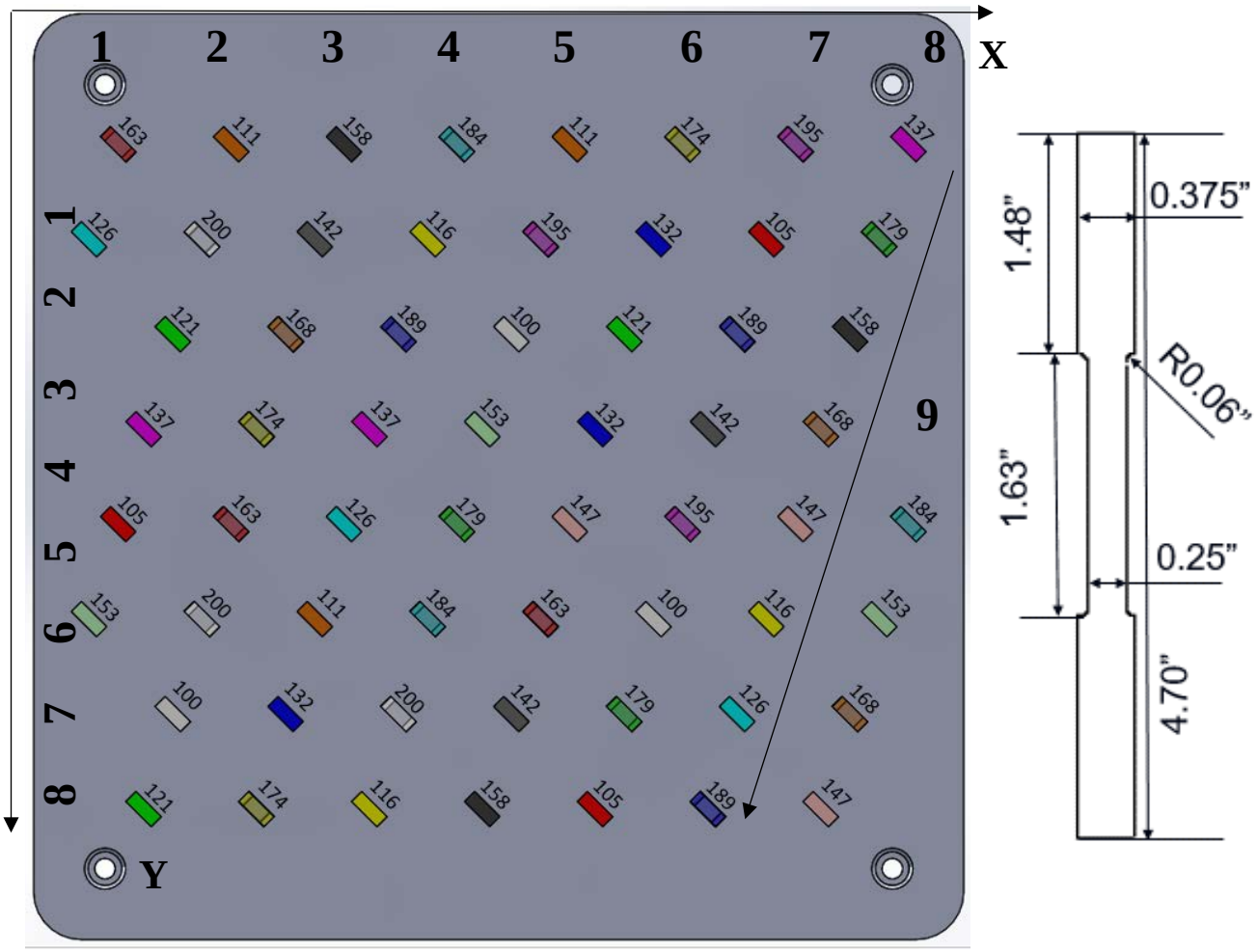

Fig. 1: Build plate layout and E8 tensile test specimen. Small annotations on the plate are the laser power; large are spatial coordinates. Note that the X coordinates are at an angle, as the directional arrow shows. All dimensions on the tensile test specimen are in inches, with a thickness of 0.15 in.

The E8 tensile test specimens were chosen because they allowed for the rapid collection of material property data and have a well-known modal response. Conceptually, the specimens can be represented as simple cantilever beams for modal analysis. The natural frequencies for a cantilever beam are given by

$$f_n = \frac{a_n^{\,2}}{2\pi}\sqrt{\frac{Ebd^3}{12mL^4}} \propto \sqrt{\frac{E}{\rho}} \qquad n=1,2,3\ldots, \tag{1}$$

where α_n is a constant that depends on the mode number, E is the Young's Modulus of the specimen, ρ is density, and b, d, L, and m are the beams width, depth, length, and mass, respectively [12]. For geometrically identical specimens, the geometry components can be factored out, making the natural frequency only dependent on the material properties of Young's Modulus and density.

Figure 2 shows a photograph of the experimental setup used to extract frequency information from the tensile test specimens. The entire build plate was attached to a shaker table supported by air bearings to allow for free vibration, and then driven with an electrodynamic shaker with a sine-chirp sweep from 0-2048 Hz. A Laser Doppler Vibrometer (LDV), along with several accelerometers and force transducers, measured the vibrational response of each individual tensile test specimen on the build plate. This vibrational data was then accumulated over the whole frequency spectrum to create a Frequency Response Function (FRF). [13].

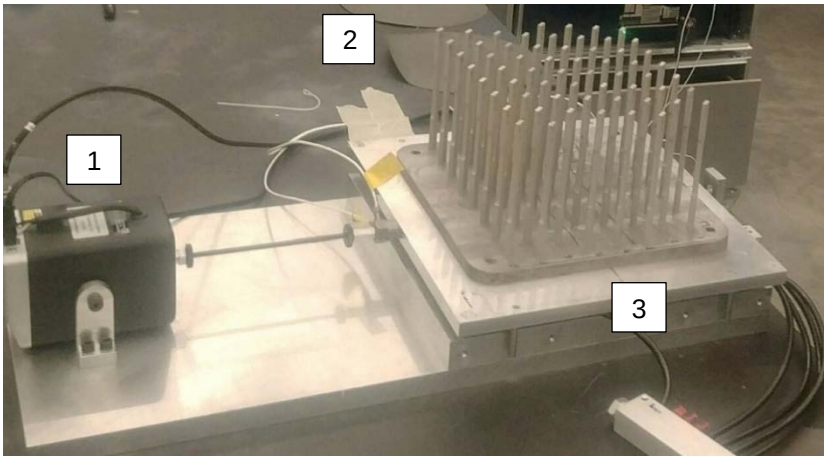

Fig. 2: Experimental setup of the 60 tensile specimens on a single plate. (LDV not shown). Points of interest: 1. Driving electrodynamic shaker. 2. Build plate with tensile specimens, attached to driven plate. 3. Manifold for air bearings, located under the plate.

In traditional modal testing, it can be a challenge to properly fixture specimens without distorting certain modes. One of the benefits of using this method is that each specimen is pre-fixed to the build plate. By adjusting the orientation of the part and support structure, almost any desired mode can be measured. Another advantage of this method is that since each part is fixed to a single piece, an entire build plate full of specimens can be tested at one time, further improving the efficiency of this method.

3. Results and Discussion

Figure 3 shows typical FRFs extracted from the LDV analysis for specimens produced with laser powers of 100, 147 and 200 W. Each FRF point represents an amplitude of response for each frequency in the tested frequency domain. Each peak represents a natural mode in the system, where a peak is associated with a response that is at least an order of magnitude higher than the surrounding noise. Finite Element Analysis (FEA) simulations performed in ANSYS predicted there are three modes under 2048 Hz (at approximately 200, 400, and 1250 Hz.) The experimentally obtained FRF's were divided into three sections using those frequencies as guidelines. The highest amplitude frequency response within a given range was selected as that modes natural frequency. The mode shapes, predicted by ANSYS, for the three modes are plotted next to the corresponding frequency ranges.

A clear frequency shift between the low power specimens and the higher power specimens was observed. This is particularly true for the third mode. It is important to note that there are a few "false modes" in the FRFs, such as the peaks at around 220 Hz in Fig. 3(b). These peaks are caused by build plate coupling. When specimens vibrate on a plate, their vibrational energy transfers down the part into the build plate. When two specimens with similar natural frequencies (within 1% of each other) vibrate out of phase with each other, their energy destructively interferes with each other, reducing vibrational responses, producing a dip in the FRF. When the specimens vibrate in phase with each other, the vibrational energy within the plate sharply rises due to resonance, forming a secondary mode, which is what is seen in the FRF [14]. The strength of this response is dependent on how well the build plate couples to the specimen which can be affected by the build plate material and geometry. Because these secondary modes are a function of the build plate geometry, they do not represent the modal responses of individual specimens and were not considered in this study. If necessary, coupling effects could be mitigated by adding temporary mass to the other specimens to shift their frequencies away from the specimen being tested.

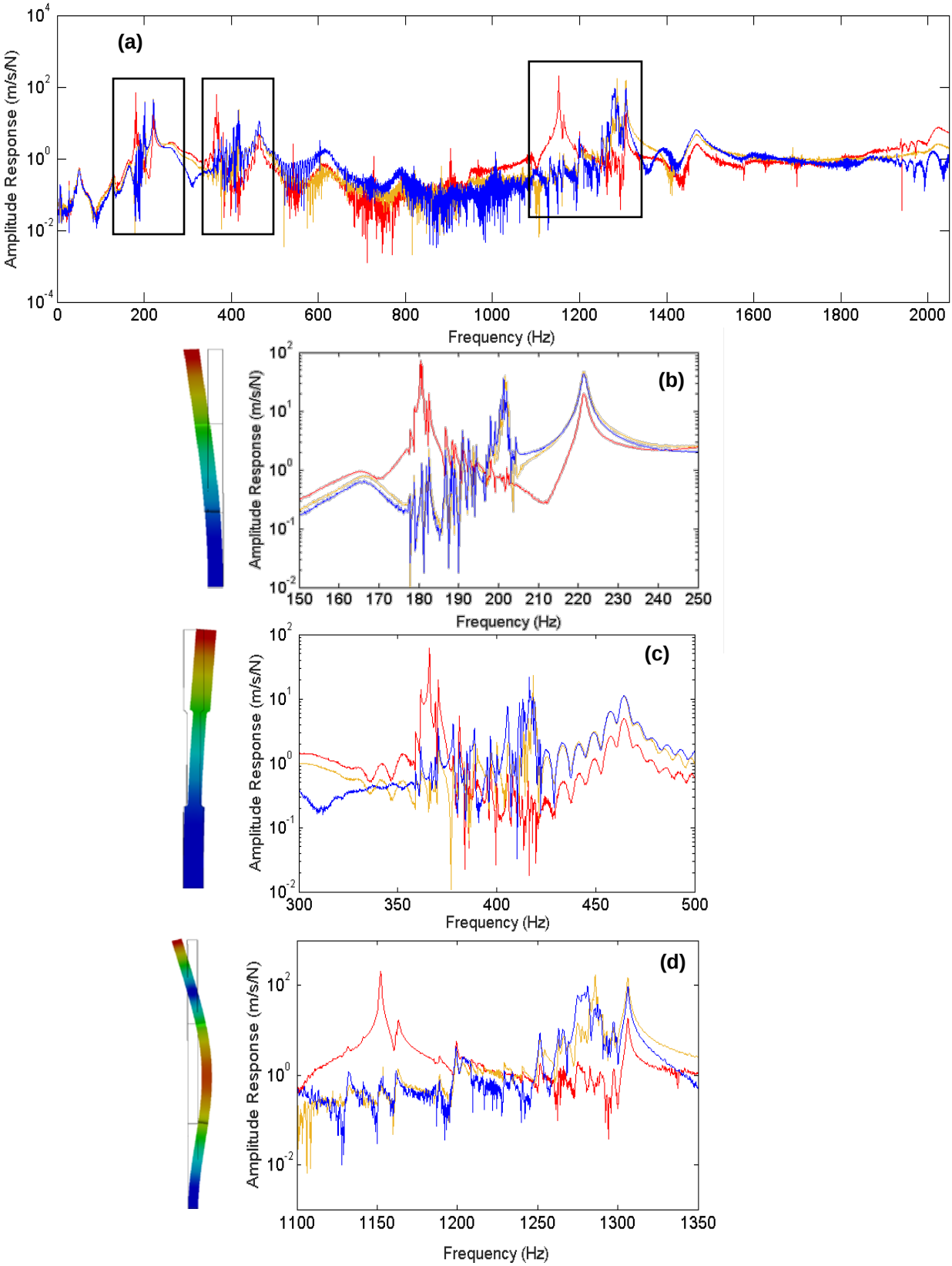

Fig. 3. Representative FRFs for various powers; red: 100 W (5,3), orange 147 W (6,5), blue: 200 W (2,2). (a) Full spectrum, (b) 1st mode, (c): 2nd mode and (d) 3rd mode.

Figure 4 shows the measured engineering properties as a function of laser power that was used to build the specimens. The material properties all appear to have a quadratic relationship to power, with each property peaking at around 170 W, with the properties decreasing for lower and higher powers.

The decrease in yield strength associated with higher input power has been noted in other material property studies, particularly in casting [4,5]. Increasing the temperature of the liquid metal too much before cooling increases the amount of time it takes for the material to recrystallize. This causes direct changes to the microstructure, such as increased grain size, which has been shown to have negative effects on the engineering properties of a material [4,5].

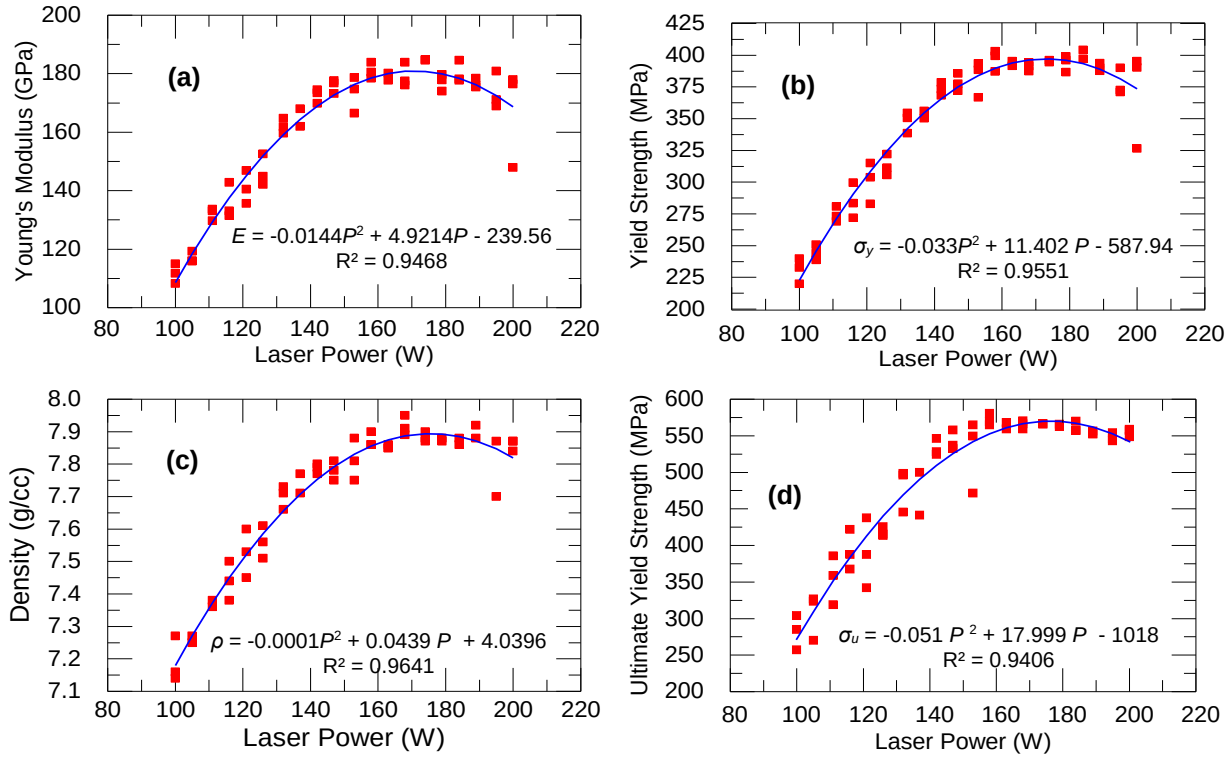

Fig. 4. Material properties versus laser power. (a) Young's modulus; (b) Yield strength (c) density; (d) Ultimate tensile strength.

Conceptually, specimens produced with lower power have a more rapid solidification of the metal. This increases the modulus due to the smaller grain size, which increases the part's strength [5]. From Eq. 1, the increased modulus (stiffness) should increase the natural frequency. However, lower power also results in higher porosity which reduces the density. The increased porosity will also increase the number of locations where dislocations and cracks form, reducing both the stiffness and the density of the material, following Eq. 1.

Figure 5 shows micrographs collected from specimens with laser powers of 100, 147, and 200 W. As shown by the density tests, specimens printed with lower powers have much greater porosity than the specimens printed at higher powers. At higher powers, however, the differences become entirely microstructure based, such as varying grain sizes, phases present, and phase constituency. Through optical or scanning electron microscopy analysis, it is possible to relate

these microstructure parameters to the engineering parameters and thermal history, forming a more complete relationship between all three parameters.

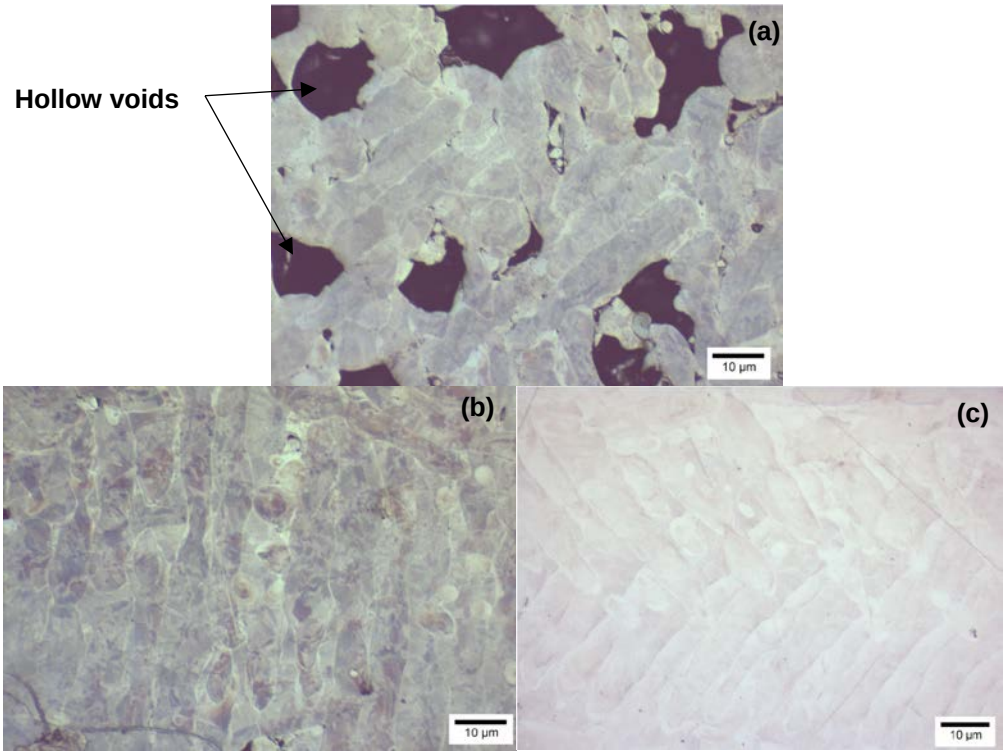

Fig. 5: Micrographs of specimens printed with varying laser powers (a) 100 W, (b) 147 W, (c) 200 W

Figure 6 shows the first three natural frequencies as a function of laser power. The natural frequencies follow a very similar pattern to that of the material properties, with a quadratic relationship. This relationship agrees with Eq. 1 assuming that all the specimens are geometrically identical. Figure 4 showed that Young's modulus decreases at a rate at least two orders of magnitudes greater than density so this dominates the frequency response.

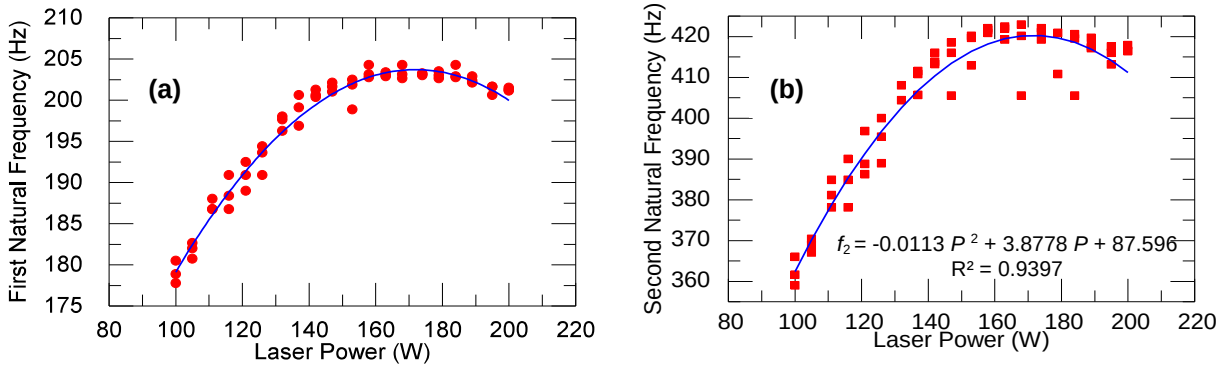

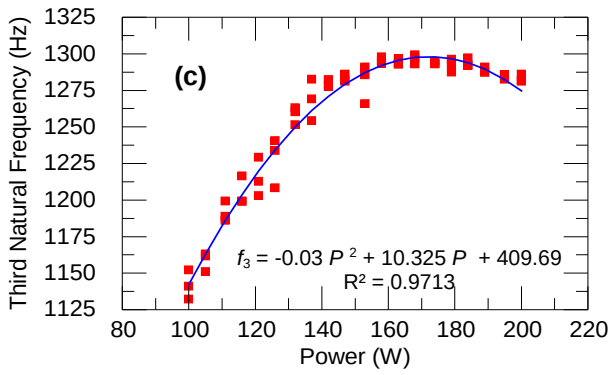

Fig. 6: Part Natural Frequency versus applied power for (a) 1st, (b) 2nd and (c) 3rd modes.

Both the engineering properties and natural frequencies scale quadratically with the laser power. Figure 7 plots the yield strength against the first three natural frequencies and shows a linear relationship. Similar relationships were found for Young's modulus and ultimate tensile strength, but are not shown here.

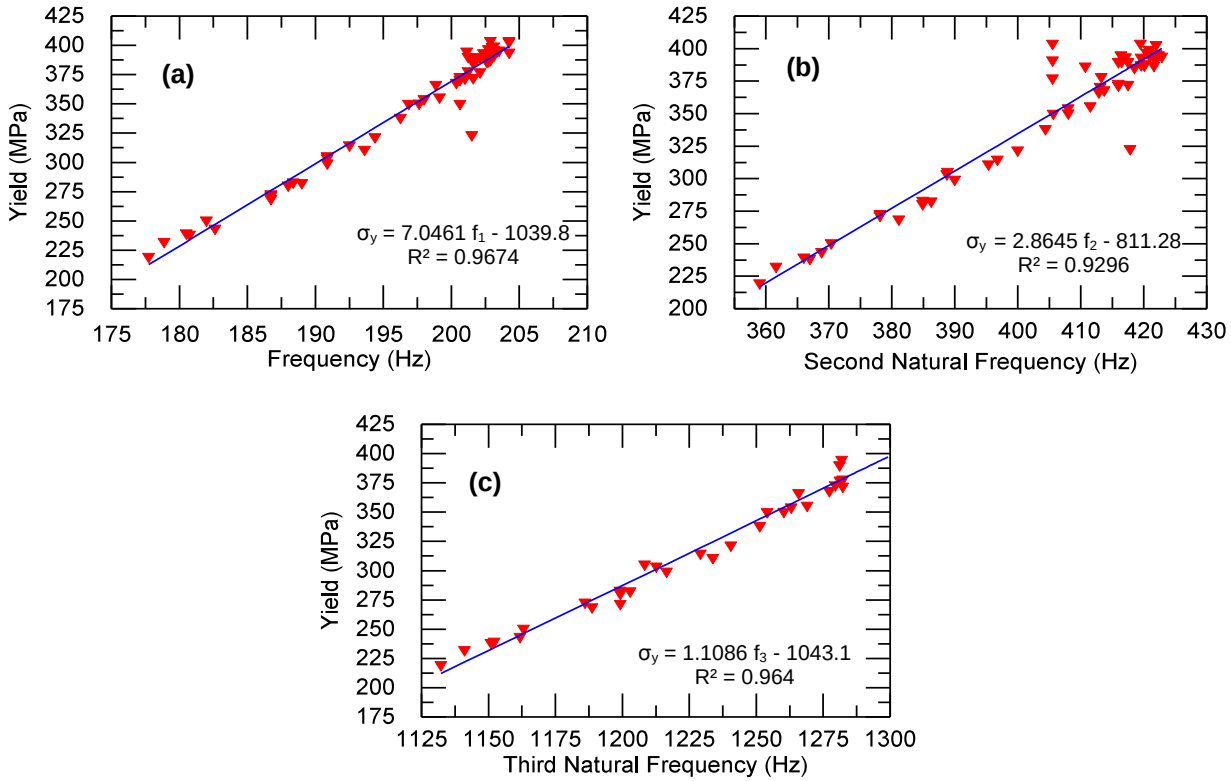

Fig. 7. Yield strength versus natural frequencies of (a) 1st, (b) 2nd, and (c) 3rd modes.

In addition to frequency relationships, it is also possible to correlate the Young's modulus directly with density. For parts that are not fully dense, the modulus of an AM part is dependent on its density [15],

$$E = E_0 \exp(-bP) \tag{2}$$

where E is the elastic modulus of the porous specimen, E_0 is the nominal modulus (found experimentally), P is the percentage volume porosity of the material, and b is a material constant that can be found through fitting experimental data.

For materials that are considered isotropic, the volumetric and area porosities are identical, and can be represented by

$$P = \frac{A_{Empty}}{A_{Tot}} = \frac{V_{Empty}}{V_{Tot}} \tag{3}$$

For geometrically identical samples, the relative density can be found by dividing the experimental density of the whole part by the theoretical maximum density (Eq. 4). For the 304L stainless steel test specimens, it was found that the maximum density was 7.95 g/cc.

$$\rho_{Rel} = \frac{\rho_{Exp}}{\rho_{Max}} P = \frac{A_{Empty}}{A_{Tot}} = \frac{V_{Empty}}{V_{Tot}} \tag{4}$$

where the p_{Exp} is found through the Archimedes principle, [4].

$$\rho_{Exp} = \frac{M_{Air}}{M_{Air} - M_{Fl}} * \rho_{Fl} \tag{5}$$

where M_{Air} is the mass of the specimen in air, M_{Fl} is the mass of the specimen in the measured fluid, and p_{Fl} is the density of the fluid. For this experiment, deaerated water at 20° C was used, which has a density of 0.9982 g/cc. After solving for the relative density in Eq. 4, it is possible to relate the relative density directly to the porosity of the material; P=1-ρ_{Rel}. It is important to note that the porosity-density relationship assumes all internal voids are hollow and have negligible mass. Figure 8 shows Young's modulus as a function of the volumetric porosity (Eq. 2).

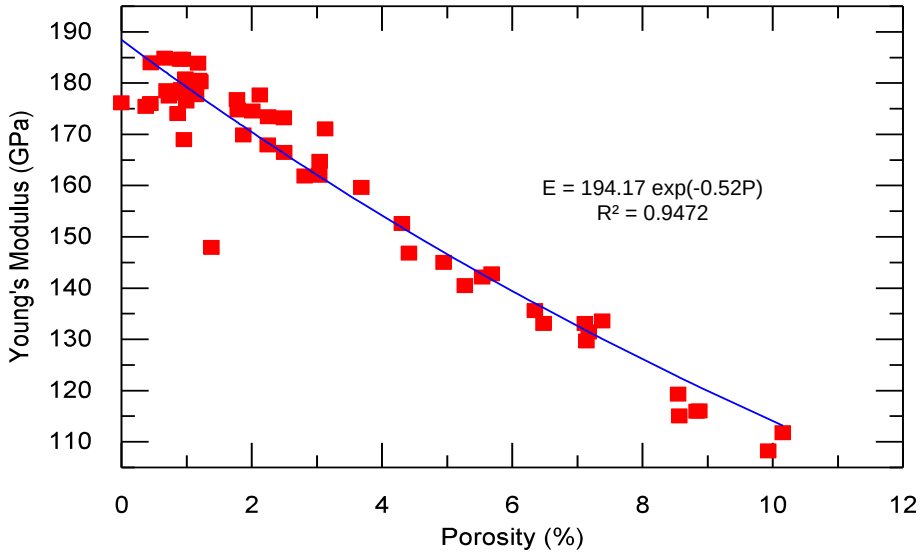

Fig. 8: Young's modulus vs volumetric porosity with secondary fit

4. Summary and Conclusions

This paper presents results from 60 tensile test specimens created using an SLM process with various laser powers. These changes in process parameters modified many aspects of the parts, including the density, Young's modulus, and yield and ultimate strengths. The changes in these features, particularly Young's modulus and density, produced shifts in the modal response of the specimens. Using frequency information extracted through modal analysis, and material property information gathered from density and tensile testing, it was shown that a direct correlation exists between the processing parameters of an AM part and its material properties.

These findings suggest that it is possible to use modal analysis to quantifiably measure changes in the material properties of a part, which could effectively be used to identify parts with sub-optimal strengths. Among many potentially applications, the method presented could benefit the AM industry by being used as a prescreening method for identifying excessively weak parts before being verified by another method, such as CT scanning, reducing time and cost.

Future work will consist of refining this study in an attempt to identify point defects in a part, where point defects refer to distinct damages in the part, such as a large internal void, crack, or delamination. The ultimate goal is to develop a validation methodology capable of detecting damages in geometrically complex parts produced by AM processes.

5. Acknowledgements

The authors gratefully acknowledge the financial support from the National Science Foundation (EEC–1461102) and KC-NSC PDRD.

6. References

[1] Gao W, Zhang Y, Ramanujan D, Ramani K, Chen Y, Williams CB, et al. The status, challenges, and future of additive manufacturing in engineering. Computer-Aided Design. 2015; 69:65-89.

[2] Frazier WE. Metal additive manufacturing: A review. Journal of Materials Engineering and Performance. 2014; 1917-28.

[3] Bontha S, Klingbeil NW, Kobryn PA, Fraser HL. Effects of process variables and size-scale on solidification microstructure in beam-based fabrication of bulky 3D structures. Materials Science and Engineering: A. 2009; 513:311-8.

[4] Gu H, Gong H, Pal D, Rafi K, Starr T, Stucker B. Influences of energy density on porosity and microstructure of selective laser melted 17-4PH stainless steel. Solid Freeform Fabrication Symposium; 2013.

[5] Hall EO. The deformation and ageing of mild steel: III discussion of results. Proceedings of the Physical Society. Section B. 1951; 64(9):747.

[6] Van Bael S, Kerckhofs G, Moesen M, Pyka G, Schrooten J, Kruth JP. Micro-CT-based improvement of geometrical and mechanical controllability of selective laser melted Ti6Al4V porous structures. Materials Science and Engineering: A. 2011; 528(24):7423-31.

[7] Banhart J. Manufacture, characterisation and application of cellular metals and metal foams. Progress in materials science. 2001 Dec 31;46(6):559-632.

[8] Schwarz BJ, Richardson MH. Experimental modal analysis. CSI Reliability week. 1999; p. 1-12.

[9] Hearn G, Testa RB. Modal analysis for damage detection in structures. Journal of Structural Engineering. 1991; 117(10):3042-63.

[10] Kerschen G, Worden K, Vakakis AF, Golinval JC. Past, present and future of nonlinear system identification in structural dynamics. Mechanical systems and signal processing. 2006 Apr 30;20(3):505-92.

[11] ASTM E8/E8M-16a Standard Test Methods for Tension Testing of Metallic Materials, ASTM International, West Conshohocken, PA, 2016,

[12] Orhan S. Analysis of free and forced vibration of a cracked cantilever beam. NDT & E International. 2007; 40(6):443-50.

[13] Nassif HH, Gindy M, Davis J. Comparison of laser Doppler vibrometer with contact sensors for monitoring bridge deflection and vibration. NDT & E International. 2005; 38(3):213-8.

[14] Novotny L. Strong coupling, energy splitting, and level crossings: A classical perspective. American Journal of Physics. 2010; 78(11):1199-202.

[15] Spriggs RM. Expression for effect of porosity on elastic modulus of polycrystalline refractory materials, particularly aluminum oxide. Journal of the American Ceramic Society. 1961; 44(12):628-9.